applied sciences

MDPI

Article

Load-Type-Based Short-Term Forecasting of Residential Load Profiles Using Machine Learning

Eray Oğuz [1,2,*], Ugur S. Selamogullari [2] and İbrahim Gürsu Tekdemir [3,*]

1 Electrical Program, Electrical and Energy Department, Vocational School, İstanbul Gedik University, Istanbul 34876, Turkey
2 Electrical Engineering Department, Faculty of Electrical and Electronics Engineering, Yıldız Technical University, Istanbul 34220, Turkey; selam@yildiz.edu.tr
3 Department of Electrical and Electronics Engineering, Faculty of Engineering and Natural Sciences, Bursa Technical University, Bursa 16310, Turkey
* Correspondence: eray.oguz@gedik.edu.tr (E.O.); ibrahim.tekdemir@btu.edu.tr (İ.G.T.)

Abstract

Accurate short-term forecasting of residential electricity demand is increasingly important for smart distribution systems, particularly in the context of demand-side management and flexibility-oriented grid operation. In this study, a high-resolution forecasting framework is proposed in which household electricity demand is classified into fixed, shiftable, and adjustable load categories and forecasted together with total load. A one-minute-resolution synthetic residential load dataset is generated using the Centre for Renewable Energy Systems Technology (CREST) demand model for households with two to five occupants over a 31-day winter period in January. The appliance-level demand data are grouped according to operational characteristics and integrated into a representative four-bus distribution feeder. Minute-level power flow analysis is then performed to calculate technical losses, which are incorporated into the forecasting dataset together with meteorological variables (temperature, wind speed, and solar irradiance) and temporal descriptors. Using this multi-input structure, random forest (RF), support vector machine (SVM), feed-forward neural network (FFNN), and long short-term memory (LSTM) models are comparatively evaluated for the prediction of fixed, shiftable, adjustable, and total residential loads. Model performance is assessed using root mean square error (RMSE) and Pearson correlation coefficient (R), while mean absolute error (MAE) is additionally reported for the final test set. The results show that the LSTM model provided the most consistent overall forecasting performance, particularly for shiftable, adjustable, and total load estimation, while RF yielded competitive results for fixed-load correlation and short-window forecasting in Buses 1 and 2. In contrast, SVM and FFNN exhibited weaker generalization performance across several load categories. The proposed framework provides a practical foundation for the development of dynamic pricing mechanisms that consider load-type-based controllability levels. Overall, the findings demonstrate that integrating load categorization with meteorological, temporal, and technical loss information provides a robust and reproducible framework for smart grid applications such as demand-side management, peak load mitigation, and flexibility-aware residential load analysis.

Keywords: short-term load forecasting; residential load classification; machine learning; LSTM; demand-side management; smart grids; multi-output forecasting

Academic Editor: Rui Araújo

Received: 25 April 2026
Revised: 21 May 2026
Accepted: 4 June 2026
Published: 11 June 2026

1. Introduction

The inherent variability of residential electricity consumption, coupled with the accelerating integration of renewable energy sources into distribution networks, presents substantial challenges for modern grid operations. These complexities often manifest as increased energy losses, voltage instabilities, and heightened uncertainty within demand-side management frameworks [1,2]. Consequently, precise short-term load forecasting (STLF) has emerged as a fundamental prerequisite for smart grids, playing a vital role in maintaining system reliability, ensuring economic efficiency, and facilitating proactive demand-side strategies [1–3].

Traditional load forecasting approaches often focus on estimating total demand profiles without explicitly considering the heterogeneous nature of residential loads [1,4]. Nevertheless, household electricity consumption is composed of diverse appliances, each characterized by distinct operating behaviors, user-driven patterns, and varying degrees of controllability [5,6]. Overlooking this diversity inherently limits the efficacy of advanced grid strategies, such as demand response (DR), load shifting, peak shaving, real-time energy management, and dynamic pricing, which rely on a more granular understanding of consumption dynamics [5,6].

To overcome these challenges, an increasing number of studies have focused on residential electricity demand modeling using machine learning and deep learning techniques. In this context, several comprehensive studies have reviewed the state of the art in residential load forecasting. For instance, Rodrigues et al. [7] provided a comprehensive review of AI-based short-term residential load forecasting methods, while Patsakos et al. [8] examined deep learning approaches for building energy forecasting and highlighted the growing research interest in residential applications. Building upon these developments, other studies have focused on improving prediction accuracy through advanced modeling techniques. For example, Moradzadeh et al. [9] demonstrated that hybrid machine learning models can significantly improve residential load prediction accuracy. In addition to these modeling approaches, residential loads are commonly categorized based on their operational characteristics. In this context, fixed loads typically represent continuously operating appliances or those independent of immediate user intervention.

While fixed loads typically represent continuously operating appliances or those independent of immediate user intervention, shiftable loads refer to time-flexible devices (e.g., washing machines and dishwashers). Conversely, adjustable loads encompass power-controllable and temperature-dependent appliances, including electric heaters and water boilers [5,6]. This classification is essential for capturing the heterogeneous and flexible nature of residential electricity consumption, which plays a critical role in demand-side management applications. Similar classifications of residential loads into rigid and flexible categories have been widely adopted in the literature to support demand response applications [10]. Such a classification enables a more realistic modeling of consumer flexibility, thereby enhancing the overall efficacy of demand response strategies [5,11]. In this context, several studies have utilized detailed bottom-up residential load models to analyze demand-side flexibility under different operational conditions and pricing schemes [12]. Similarly, Sharma et al. [13] emphasized that residential load profiling and demand-side management strategies play a critical role in improving demand response effectiveness.

Despite these advances, obtaining high-resolution residential load data at scale remains a significant challenge due to privacy concerns and limitations in metering infrastructure. Although bottom-up approaches provide high prediction accuracy by modeling residential consumption patterns, their practical implementation is often constrained by the lack of detailed real-world data [14]. Recent studies further emphasize that access to high-

https://doi.org/10.3390/app16125904

resolution household data is increasingly restricted due to privacy regulations, limiting the availability of real-world datasets [15].

To address this limitation, synthetic residential load generation has emerged as a viable alternative. Bottom-up modelling approaches, which construct load profiles based on appliance usage patterns and occupant behavior, have been widely adopted due to their ability to realistically represent residential consumption characteristics [12,15,16]. These methods are designed to preserve statistically realistic variability and peak demand behaviors, ensuring that the generated profiles remain representative of actual consumption patterns [17–19]. Recent studies have proposed forecasting approaches that do not rely on complete historical load profiles, instead leveraging synthetic features, socio-economic indicators, and weather data to estimate residential energy demand [20]. However, these approaches generally focus on aggregated load prediction rather than categorized residential load components.

Despite these advancements, several critical gaps persist in the current literature. First, a vast majority of existing studies rely on either low-resolution or consolidated load data, often centering their analysis on a single bus or the system level; consequently, the spatial diversity inherent in distribution networks is frequently overlooked [1,4,21,22]. Furthermore, load type estimation is commonly treated as a post-processing task rather than being directly integrated within a unified multi-output forecasting framework [11,23]. Although multi-input multi-output forecasting models have been explored in the literature [24], their application to categorized residential load components remains limited.

Lastly, the impact of meteorological variables, temporal information, and technical losses on categorized residential loads has not been sufficiently explored. Previous studies have demonstrated that residential load profiles are strongly influenced by user bahavior, weather conditions, and load characteristics [16]. However, the combined impact of these factors on categorized residential load components has not been sufficiently investigated. This lack of investigation is particularly evident in studies requiring minute-level resolution [25]. Although recent studies have explored ultra-short-term forecasting using minute-level data [26], these approaches primarily focus on aggregated load prediction rather than categorized residential load components.

While the analysis of technical losses and loss sensitivity in distribution systems has been extensively documented, such studies primarily adopt a grid operation or planning perspective. Consequently, they often fail to integrate these analyses with high-temporal-resolution load forecasting that accounts for categorized residential loads [25]. Furthermore, despite the well-established role of power-flow-based analyses in understanding network behavior, there is a notable scarcity of research that bridges these analytical techniques with data-driven load forecasting models [2].

Motivated by the aforementioned research gaps, this paper proposes a comprehensive residential load forecasting framework characterized by explicit load categorization and high temporal resolution. The primary contributions of this work are listed as follows:

- Generation of High-Fidelity Synthetic Data: Utilizing the CREST demand model for a winter reference period, a large-scale, minute-resolution residential load dataset is synthesized. This dataset accounts for four distinct distribution buses with heterogeneous household populations [19,27].
- Systematic Load Classification: Residential electricity demand is structured into fixed, shiftable, and adjustable categories based on appliance operating characteristics, thereby enabling a more realistic representation of demand flexibility.
- Unified Multi-Input Multi-Output (MIMO) Architecture: By integrating meteorological variables, temporal features, bus-specific indices, and network technical losses, a holistic forecasting framework is developed to simultaneously predict fixed, shiftable, adjustable, and total load components.

- Comparative Algorithmic Benchmarking: Four prominent machine learning and deep learning architectures, specifically random forest, support vector machines, feedforward neural networks, and long short-term memory networks, are deployed and rigorously evaluated under identical operational conditions.
- Strategic and Practical Insights: The proposed framework provides critical insights into the suitability of various predictive models for categorized residential loads, offering actionable implications for demand response planning and the optimization of smart distribution systems.

Although some load-classification-based forecasting frameworks have been reported in the literature, the existing studies generally do not combine load-type-based forecasting with minute-level resolution, multi-bus distribution system representation, and power-flow-derived technical loss information within a single unified framework. Therefore, the present study positions its contribution at the framework level rather than at the level of proposing a new standalone forecasting algorithm. This integrated structure provides a more application-oriented basis for demand side management, flexibility-aware grid applications, and dynamic pricing applications.

The remainder of this paper is organized as follows: Section 2 presents the dataset generation process and the methodology for load categorization. Section 3 describes the forecasting models and their training procedures. Section 4 discusses the simulation results and comparative performance analysis. Finally, Section 5 concludes the paper and outlines future research directions.

2. Data Preparation

2.1. Residential Load Dataset Generation Process

The residential load data used in this study are generated using the CREST demand model, wich enables the creation of high-resolution synthetic load profiles by capturing sthocastic household electricity consumption behavior [19,27]. A brief overview of the CREST model is provided here, focusing on aspects relevant to the proposed framework. Detailed descriptions of the model structure, appliance-level modeling, and underlying assumptions are presented in Appendix A.

The generated dataset accounts for temporal variations such as weekdays, weekends, and seasonal effects to ensure realistic demand patterns. Load profiles are produced at a one-minute resolution and aggregated to represent total residential demand. Furthermore, the aggregated loads are categorized into fixed, shiftable, and adjustable components based on appliance characteristics and operational flexibility. The procedural flow, starting from appliance-level data generation to load type aggregation and per-bus consolidation, is illustrated in Figure 1.

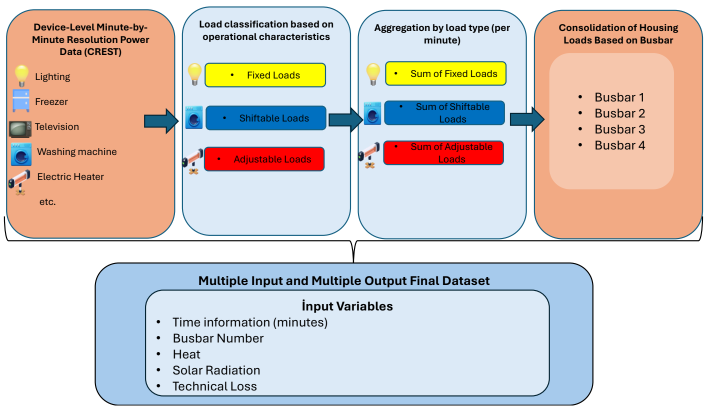

Figure 1. Schematic representation of the load type aggregation and dataset construction process.

The generated residential load profiles are integrated into four distinct buses defined within the Civanlar distribution system, a benchmark model frequently utilized in the literature.

This four-bus distribution structure is based on the well-known Civanlar test distribution system, which has been widely adopted in the literature for distribution system analysis [28,29]. It is designed to represent different residential density levels and load diversity scenarios. Each bus corresponds to a distinct aggregation level of residential loads, enabling the modeling of heterogeneous consumption patterns across the network.This design choice ensures that the scenario is not arbitrary, but grounded in a widely accepted benchmark framework.

This simplified configuration provides a flexible and controlled framework for evaluating forecasting performance under varying load conditions, rather than replicating a specific real-world distribution feeder in detail. By incorporating different load distributions across buses, the proposed framework allows for the assessment of model robustness under diverse demand scenarios [28,29].

To determine the number of households allocated to each bus, target active power values are established as a baseline. For this purpose, the average instantaneous power consumption of households with two to five occupants are calculated, defining a representative residential group where each household type is equally represented. Under this configuration, the household counts for the first, second, third, and fourth buses are set at 3492, 5240, 3492, and 2620, respectively. The total power value designated for each bus is divided by the average instantaneous consumption of this group to derive the required number of units, with the total residential count calculated based on groups comprising four households each. This allocation procedure is independently executed for all buses. The topology of the distribution system and the specific bus structures employed in this study are illustrated in Figure 2. Residential loads were assigned to the defined buses within this system in an aggregated basis.

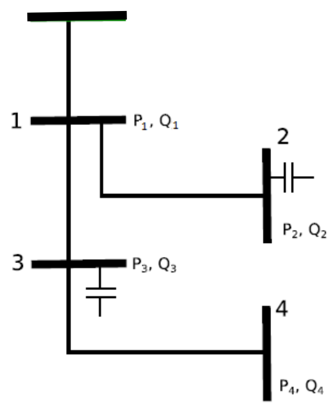

Figure 2. Detailed single-line diagram of the distribution test system utilized in this study [28,29].

The CREST model is executed for a one-month duration, from 1 January to 31 January, to capture the distinct behavioral patterns of both weekdays and weekends. Accounting for the four distribution buses and a 31-day period at minute-level resolution, the resulting dataset comprises a total of 178,560 observations. Each record signifies the totalized electricity demand for a specific bus at a given minute-level timestamp. An illustrative example of the generated dataset is presented in Figure 3, which depicts the time-series profiles of fixed, shiftable, and adjustable load components for Bus 3 on 20 January. As can be observed, the CREST model effectively captures the temporal variability and diversity of load characteristics throughout the day.

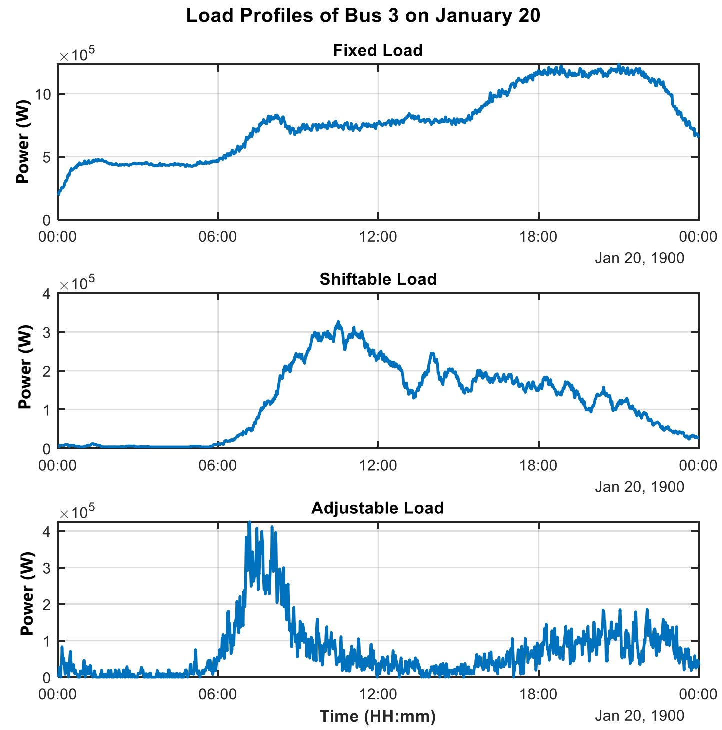

Figure 3. Fixed, shiftable, and adjustable load profiles of Bus 3 on 20 January generated using the CREST model.

2.2. Classification of Residential Loads by Operational Type

In order to accurately reflect the heterogeneous nature of residential electricity consumption and its potential for demand-side flexibility, the total load is partitioned into three categories: fixed, shiftable, and adjustable. This classification is executed by evaluating the operational characteristics and controllability levels of household appliances, ensuring full alignment with established demand-side management frameworks in the literature. Furthermore, this classification supports recent appliance-level load modeling studies that emphasize the diverse operating characteristics of household appliances [30,31].

As shown in Figure 4, the CREST model generates appliance-level electricity consumption data at a one-minute resolution. These appliance-level loads are aggregated to obtain total residential demand.

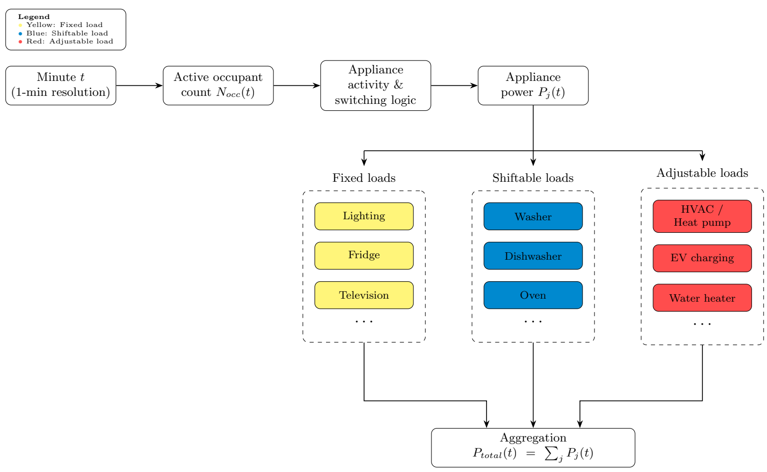

Figure 4. Example of minute-resolution appliance-level residential load data generated by the CREST model.

The aggregated demand is categorized into fixed, shiftable, and adjustable load components, enabling the analysis of different load types within the forecasting framework.

2.3. Input Feature Construction

The input variables utilized for the load forecasting models are not confined to historical load values alone; instead, the dataset is augmented with supplementary predictors representing environmental and network conditions. Climatic parameters, in particular, exert a significant influence on residential electricity demand, primarily through their impact on temperature-dependent space heating loads [32].

Since the CREST model does not inherently generate meteorological data, weather-related variables are sourced from external repositories. Ambient temperature, wind speed, and solar radiation data are retrieved from the Open-Meteo platform [33] for the corresponding time period. To ensure consistency, these variables are downsampled or interpolated to a one-minute resolution and temporally aligned with load data time series.

In addition, power flow analyses are conducted for each discrete time step to quantify the technical losses of the distribution system. The Civanlar distribution network model is adapted within the MATLAB R2023a (MathWorks, Natick, MA, USA) environment to calculate line losses to derive technical loss values in megawatts (MW). These computed losses are subsequently embedded within the feature matrix as an auxiliary input feature.

Consequently, a comprehensive set of input features is established for each discrete time step, encompassing both environmental variables and system-specific parameters. The finalized input matrix incorporates the following features:

- Date index;
- Minute-of-day information;
- Bus identification number;
- Ambient temperature;
- Wind speed;
- Solar irradiance;
- Technical loss value;
- Day-of-month index;
- Month index.

This formulation defines a multi-input, multi-output (MIMO) forecasting framework, in which all four load components are predicted simultaneously. This structure enables the models to capture both individual load dynamics and their collective behavior under varying environmental and system conditions.

2.4. Data Preprocessing and Normalization

Prior to model training, all generated time series undergo a rigorous preprocessing to ensure computational compatibility. Initially, data from heterogeneous sources are temporally aligned, and the resulting sequences are scrutinized for missing or inconsistent data. Given that the input and output variables span diverse numerical scales, a min-max normalization technique is applied to scale all values within the [0, 1] range. This transformation is executed to enhance the numerical stability and convergence efficiency of the learning process.

The dataset is partitioned into training, validation, and testing subsets using a chronological splitting strategy in order to preserve the temporal structure of the time series data. Specifically, 70% of the data are allocated for training, 15% for validation, and 15% for testing. Random shuffling is not applied, ensuring that all models are evaluated on future

https://doi.org/10.3390/app16125904

unseen data segments. This approach provides a more realistic assessment of forecasting performance in practical deployment scenarios.

The resulting data structure provides a comprehensive basis for a multi-input, multi-output (MIMO) forecasting framework, enabling the simultaneous prediction of fixed, shiftable, adjustable, and total load profiles.

3. Methodology

The overall workflow of the proposed method is presented in Figure 5. The previous section explains the data preparation and preprocessing procedures. In this section, the forecasting models and evaluation metrics are described. To ensure a consistent and fair comparison between different forecasting approaches, all models are developed under an identical experimental framework. Specifically, the same input-output structure, dataset, and chronological training/validation/testing partition are employed across all methods. In addition, all input and output variables are normalized using parameters derived exclusively from the training dataset to prevent data leakage. While the forecasting task is formulated as a multi-input, multi-output (MIMO) problem, the implementation strategy differs across models: tree-based and kernel-based methods (RF and SVM) are constructed as independent single- output regressors for each output variable, whereas FFNN and LSTM models are designed to predict all load components simultaneously. Hyperparameters for each model are selected based on commonly reported ranges in the literature and further refined using validation set performance.

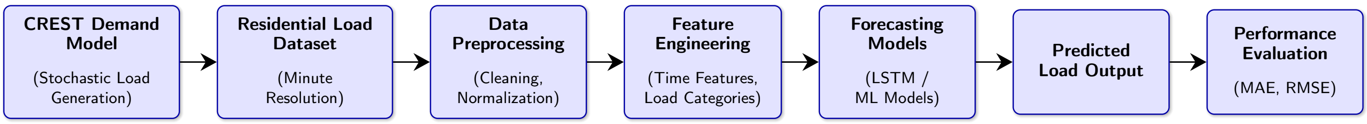

Figure 5. Overall workflow of the proposed residential load forecasting framework.

3.1. General Forecasting Framework

In this study, the main focus is the independent estimation of fixed, shiftable, adjustable, and total load components for each discrete time interval. To this end, the research problem is formulated as a multivariate regression task characterized by complex, nonlinear relationships. All forecasting models are uniformly trained and validated using an identical dataset and a consistent input-output architecture. This approach ensures an objective benchmarking of the performance across various artificial intelligence techniques. The underlying dataset comprises the aggregated load components generated through the previously detailed preprocessing phase, maintained at a one-minute temporal resolution.

The model inputs consist of a multifaceted set of temporal, environmental, and grid-related variables that influence residential electricity demand. Specifically, these predictors include the date index, minute of day information, bus identification number, ambient temperature, wind speed, solar irradiance, technical loss value, day of month index, and month index for the corresponding time step. This structure enables the model to learn the variations of load types not only from historical consumption values but also from external environmental conditions and network states. The forecasting procedure adopted in this study is given in Figure 6.

Although the forecasting problem is formulated as a multi-output task, tree-based (RF) and kernel-based (SVM) methods are implemented as independent single-output regressors for each load component. In contrast, FFNN and LSTM models are trained in a fully multi-output configuration, enabling them to learn cross-correlations between load categories.

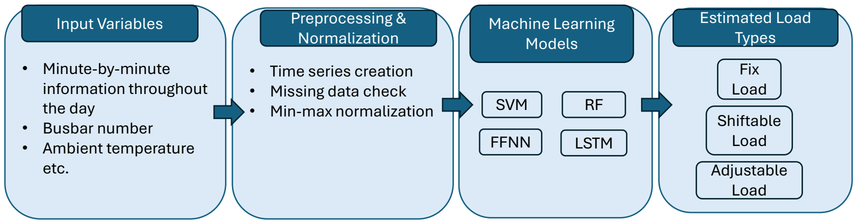

Figure 6. Steps of the forecasting procedure adopted in this study.

The model outputs comprise the consolidated power consumption values for fixed, shiftable, adjustable, and total loads corresponding to the same time step. Consequently, each model operates within a multi-output architecture that facilitates the simultaneous estimation of these four output components. This approach enables the framework to effectively capture and learn potential cross-correlations between the different load types.

The dataset is partitioned into training, validation, and testing subsets for all models, with performance evaluations conducted exclusively on the test data. This approach enables a robust comparison of the models' generalization capabilities on out-of-sample data. Under this general framework, various machine-learning-based forecasting methodologies are implemented and their results subjected to comparative analysis. The input and output variables utilized across these forecasting models are summarized in Table 1.

Table 1. Summary of input features and output variables utilized in the forecasting models.

Variable Type	Variable	Description
Input	Date index	Represents the chronological position of each observation
Input	Minute-of-day index	Represents intra-day cyclic consumption patterns
Input	Bus identification number	Captures the spatial distribution of electrical loads
Input	Ambient temperature	Influences thermal heating and behavioral load variations
Input	Wind speed	Represents indirect weather-dependent consumption impacts
Input	Solar irradiance	Affects daylight-dependent activities and lighting usage
Input	Technical loss value	Reflects the operational loading state of the distribution system
Input	Day-of-month index	Represents within-month temporal variation
Input	Month index	Encodes the calendar month information
Output	Fixed load	Load component characterized by continuous operation and low flexibility
Output	Shiftable load	Load component whose operational schedule can be deferred
Output	Adjustable load	Power-controllable and temperature-sensitive load component
Output	Total load	Aggregate of fixed, shiftable, and adjustable loads

3.2. Random-Forest-Based Forecasting

Random forest (RF) is a robust machine learning methodology built upon an integrated ensemble of multiple decision trees. This approach incorporates the principle of aggregating the outputs from a multitude of trees, each trained on randomly sampled data subsets and randomly chosen feature subspaces. In the context of regression tasks, the global prediction is derived by averaging the individual predictions generated across the entire forest. Figure 7 illustrates the RF-based load forecasting infrastructure.

In this research, the RF approach is employed to estimate the fixed, shiftable, adjustable, and total load components of residential electricity demand. In implementation, this approach is realized through four independent regression models, one for each output variable. Due to its capacity for modeling complex, nonlinear mappings between input features and diverse load categories, the RF method is highly effective for representing the heterogeneous nature of household consumption patterns. Furthermore, the ensemble architecture of the RF method exhibits a structural immunity to overfitting compared to individual decision trees, thereby offering a robust alternative for enhancing generalization performance.

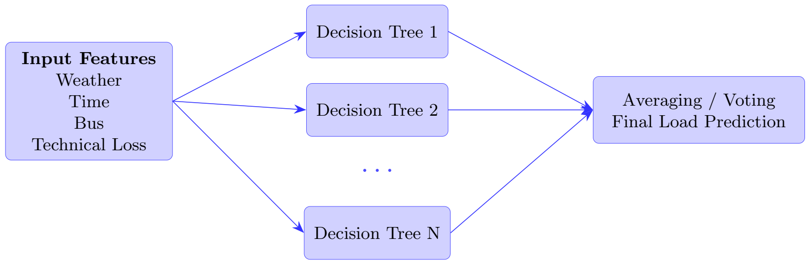

Figure 7. RF-based load forecasting structure.

The RF model is configured with 200 decision trees and a minimum leaf size of 5. These parameters are selected to balance model complexity and generalization performance while maintaining computational efficiency. By virtue of its random sampling and feature selection mechanisms, the method facilitates the extraction of complex interactions between input variables, thereby generating reliable predictions across diverse load categories. The training phase is conducted using the training subset, while the final performance assessments are executed on unused validation samples to ensure the validity of the results on previously unobserved data.

3.3. Support-Vector-Machine-Based Forecasting

Support vector machine (SVM) is a machine learning method based on statistical learning theory that provides strong generalization performance in high-dimensional data spaces. Its adaptation for regression tasks, known as support vector regression (SVR), strives to model the relationship between input and target variables by identifying the flattest possible function within a predefined error tolerance (ϵ) [34]. This approach aims to minimize structural risk by balancing model complexity against prediction error, thereby providing an inherent resilience to overfitting.

In this study, the SVM model employs a Gaussian (RBF) kernel with automatic kernel scaling. The penalty parameter is set to $C = 10$, and the insensitive loss parameter is defined as $\varepsilon = 0.1$. Input features are standardized prior to training to improve numerical stability. By using kernel functions, the input data are projected into a higher dimensional feature space, thereby enabling the indirect characterization of complex, nonlinear dependencies. This process is illustrated in Figure 8.

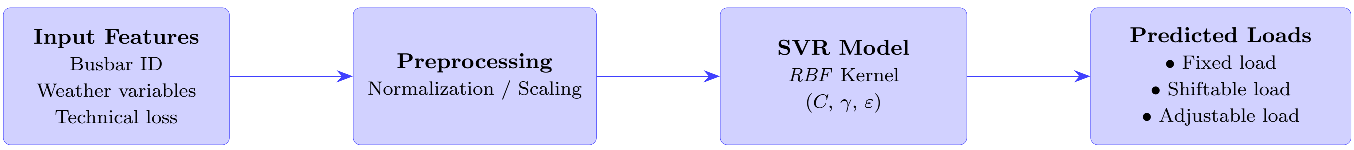

Figure 8. SVM (SVR with RBF kernel)-based load forecasting structure.

Analogous to the RF approach, four independent SVR models are trained, one for each output variable. This ensures that fixed, shiftable, adjustable, and total loads are addressed as individual predictive problems, each tailored to their unique dynamic characteristics.

The core hyperparameters of the model, specifically the penalty parameter (C), the error tolerance (ε), and the kernel parameter (γ), are methodically selected from ranges widely established in the literature. These parameters are calibrated to maintain a delicate trade off between fitting the training data and ensuring robust generalization. The training process is conducted on the training subset, while hyperparameter optimization is performed using the validation set. The final performance assessment is carried out on previously unused testing samples to ensure an unbiased evaluation.

3.4. Feedforward-Neural-Network-Based Forecasting

Feedforward neural networks (FFNNs) are multilayered computational models employed to converge upon the nonlinear mapping between input features and categorized load outputs. The FFNN architecture adopted in this research comprises an input layer, multiple fully connected (dense) hidden layers, and an output layer. The structure is illustrated in Figure 9. By virtue of the nonlinear activation functions integrated within the hidden layers, the network facilitates the extraction of complex interactions between temporal, meteorological, and spatial features, thereby effectively representing stochastic demand fluctuations.

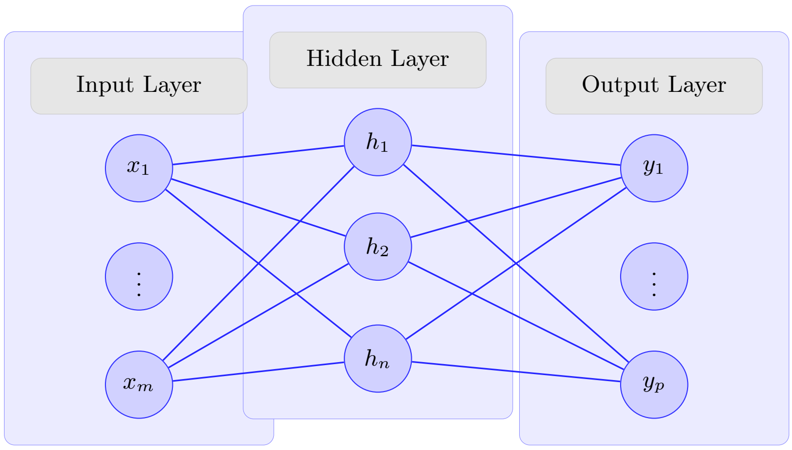

Figure 9. Feedforward neural network (FFNN) structure.

The FFNN model concurrently generates all four output variables, thereby facilitating the implicit learning of cross load interactions and latent correlations between the different load components.

The FFNN architecture consists of three hidden layers with 128, 64, and 32 neurons, respectively. The network parameters are optimized using the scaled conjugate gradient (SCG) backpropagation algorithm, which provides efficient training for medium-scale datasets. The activation functions of the hidden layers are selected as hyperbolic tangent sigmoid (tansig), while the output layer employs a linear activation function (purelin). The training process is configured with a maximum of 300 epochs, a minimum gradient threshold of 10^{-7}, and an early stopping criterion based on validation performance. This configuration enables the network to capture nonlinear relationships between input variables and load components while maintaining computational efficiency.

The FFNN model does not directly incorporate the historical values of the time series; instead, it focuses on capturing the simultaneous relationships between input variables and load components at each individual time step. Consequently, the model offers an effective approach for representing the instantaneous nonlinear mappings between electricity demand and the prevailing environmental and grid conditions. Furthermore, it serves as a standard MLP reference architecture to facilitate a rigorous comparative analysis with other machine learning and deep learning methodologies.

The model's hyperparameters, including the number of layers, neuron density, learning rate, and total epochs for training, are calibrated based on established literature benchmarks and comprehensive grid search trials. Throughout the training process, a validation subset is utilized to monitor and mitigate the risk of overfitting, while the final predictive performance is evaluated on an independent test set to ensure the model's reliability on previously unused data.

3.5. Long-Short-Term-Memory-Based Forecasting

In order to explicitly capture the temporal dependencies inherent in minute-level residential load data, a long short-term memory (LSTM) network is employed. As an advanced variant of recurrent neural networks (RNNs), the LSTM architecture is specifically engineered to mitigate the vanishing gradient issue and model long-term temporal correlations within sequential data. It is particularly distinguished by its dual capability to characterize both short- and long-term dependencies in time series [35]. Through its specialized memory cells and gating mechanisms comprising input, forget, and output gates, the LSTM effectively learns the dynamic synergy between historical information and current inputs, thereby providing a robust representation of complex temporal dynamics.

In this study, the LSTM model processes the input data using a sliding-window sequence structure in order to explicitly capture temporal dependencies in the minute-level residential load profiles. In this approach, consecutive historical observations are arranged as input sequences, and the corresponding load components are estimated at the target forecasting step. This formulation enables the LSTM network to learn short-term temporal dependencies more effectively than static regression models. The entire training dataset is provided as a sequence, allowing the network to learn temporal dependencies directly through its internal memory cells. The LSTM architecture consists of a single recurrent layer with 150 hidden units, followed by a dropout layer with a rate of 0.1, a fully connected layer with 64 neurons, and a final regression layer. The model is trained using the Adam optimizer with an initial learning rate of 0.001, a maximum of 100 epochs, a piecewise learning rate schedule, and a mini-batch size of 128. A sliding window length of 30 min is used to construct the input sequences. This architectural configuration ensures that the model accounts not only for instantaneous conditions but also for the underlying trends and trajectories embedded within prior time steps. The structure is illustrated in Figure 10.

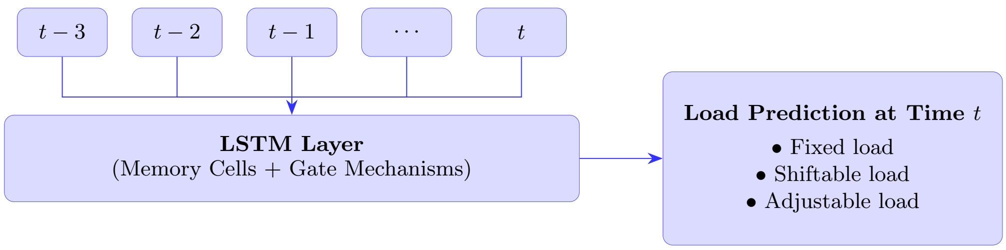

Figure 10. Sequence-based load forecasting using the LSTM model.

The LSTM architecture is configured to incorporate one or more LSTM layers, followed by a fully connected dense output layer. This output layer yields the totalized power consumption values for fixed, shiftable, adjustable, and total loads corresponding to the specific time step. Through this methodological approach, the model is capable of simultaneously learning the temporal and compositional correlations between the fixed, shiftable, adjustable, and total load components.

The network parameters are optimized using the backpropagation through time (BPTT) algorithm, an extension of backpropagation specifically designed for recurrent architectures. To ensure robust generalization, the model's performance is closely scrutinized via a validation subset, and regularization techniques such as early stopping are implemented to mitigate the risk of overfitting. Key hyperparameters, including the sliding window length, the number of LSTM layers, hidden unit density, and the learning rate, were determined through a combination of established literature benchmarks and comprehensive grid search experiments.

By leveraging its intrinsic memory cells and gating mechanisms, the LSTM model effectively captures both short-term fluctuations and long-term consumption patterns driven by the complex interplay between weather conditions and consumer lifestyle cycles. Therefore, the LSTM approach has been evaluated as a method that offers higher representational power in modeling the temporal dynamics of residential load behavior compared to other machine learning methods.

The hyperparameters for all machine learning models employed in this research are carefully derived from established ranges recommended in the literature and subsequently fine-tuned through validation set performance.

The primary hyperparameters used for each model are summarized in Table 2 to ensure transparency and reproducibility. These parameters are determined through an empirical and iterative tuning process based on validation performance.

Table 2. Primary hyperparameters employed in forecasting models.

Model	**Primary Hyperparameters**
RF	Number of trees = 200, minimum leaf size = 5
SVM	Kernel = RBF, $C = 10$, $\varepsilon = 0.1$, kernel scale = auto
FFNN	Hidden layers = [128, 64, 32], training algorithm = SCG, epochs = 300
LSTM	Sliding window length = 30 min, hidden units = 150, dropout = 0.1, fully connected neurons = 64, epochs = 100, learning rate = 0.001, batch size = 128

All models are trained and evaluated under identical conditions to ensure a fair comparison.

An examination of Table 2 reveals that while model complexity in traditional machine learning methods (RF, SVM) is primarily governed by tree depth and kernel coefficients, the performance of deep-learning-based models (FFNN, LSTM) is critically dependent on their architectural configuration, specifically the number of layers and neuron density. To ensure an unbiased benchmark across these four distinct forecasting approaches, each method is trained and validated using a homogenous dataset and an identical set of input variables.

3.6. Evaluation Metrics

The predictive performance of the proposed forecasting models is evaluated using three statistical indicators, namely RMSE, MAE, and R. These metrics are computed on the original (non-normalized) scale of the load data to ensure meaningful physical interpretation of the results.

The RMSE metric is used to quantify the magnitude of the prediction error. It represents the square root of the average of the squared differences between the predicted and actual load values, and is defined as follows:

$$\mathrm{RMSE} = \sqrt{\frac{1}{N}\sum_{i=1}^{N}(y_i - \hat{y}_i)^2} \tag{1}$$

where y_i and $\hat{y}_i$ denote the actual and predicted load values at time step i, respectively, and N represents the total number of samples. The RMSE provides a direct measure of prediction accuracy in the same unit as the load values, thereby allowing an intuitive assessment of model performance in terms of absolute error magnitude.

In addition to RMSE, MAE is used to quantify the average absolute prediction error. Unlike RMSE, MAE is less sensitive to large individual errors and therefore provides a complementary interpretation of average forecasting deviation. It is defined as follows:

$$\text{MAE} = \frac{1}{N}\sum_{i=1}^{N}|y_i - \hat{y}_i| \tag{2}$$

The Pearson correlation coefficient (R) is employed to evaluate the degree of linear association between the predicted and actual load profiles. This metric reflects the ability of the forecasting model to capture the temporal patterns and trends of the load signal, independent of scale differences. The correlation coefficient is calculated as:

$$R = \frac{\sum_{i=1}^{N}(y_i - \bar{y})(\hat{y}_i - \bar{\hat{y}})}{\sqrt{\sum_{i=1}^{N}(y_i - \bar{y})^2}\sqrt{\sum_{i=1}^{N}(\hat{y}_i - \bar{\hat{y}})^2}} \tag{3}$$

where $\bar{y}$ and $\bar{\hat{y}}$ represent the mean values of the actual and predicted load series, respectively. The value of R lies within the interval $[-1, 1]$, where values close to 1 indicate a strong positive correlation and high agreement between the predicted and actual signals.

RMSE, MAE, and R are computed separately for each load category, namely fixed, shiftable, adjustable, and total load, in order to provide a comprehensive evaluation of the forecasting performance across different demand characteristics. While RMSE reflects the magnitude of prediction errors, the correlation coefficient provides complementary insight into the model's ability to reproduce the temporal dynamics of the load profiles. Therefore, the joint interpretation of these metrics enables a more robust and balanced assessment of model performance. All performance metrics are computed after reversing the normalization process, ensuring that the reported values reflect the true physical scale of the load data.

4. Results and Discussion

The forecasting performance of the RF, SVM, FFNN, and LSTM models is evaluated under identical experimental conditions using the same dataset and a chronological training/validation/testing partition. The complete dataset consisted of 178,560 samples, of which 124,991 (70%) were used for training, 26,784 (15%) for validation, and 26,785 (15%) for testing. In order to preserve the temporal structure of the residential demand data, random shuffling is not applied. The predictive accuracy of the models is assessed using RMSE and R for validation and test comparisons. In addition, MAE is reported for the final test set to provide an additional absolute-error-based evaluation.

The validation set performance results are presented in Table 3, while the final test set results are summarized in Table 4. In general, the validation results indicate that the LSTM model provides the most stable behavior across all four outputs, particularly for fixed and total load forecasting. RF also performs competitively, especially for adjustable load. By contrast, SVM and FFNN exhibit weaker validation performance for shiftable and total load components, suggesting difficulties in capturing more irregular and event-driven consumption patterns.

The final test set results in Table 4 indicate that the LSTM model provides the strongest overall generalization capability among the evaluated forecasting methods. In particular, LSTM achieves the lowest RMSE values for shiftable, adjustable, and total load forecasting, with corresponding correlation coefficients of 0.9733, 0.9146, and 0.9901, respectively. These findings confirm that the sliding-window-based recurrent structure significantly improves the representation of temporal dependencies in minute-level residential load data, especially for load components characterized by intermittent activation behavior and accumulated temporal effects.

Table 3. Validation set performance comparison of forecasting models.

Method	RMSE (Fixed)	*R* (Fixed)	RMSE (Shiftable)	*R* (Shiftable)	RMSE (Adjustable)	*R* (Adjustable)	RMSE (Total)	*R* (Total)
RF	170,477	0.9382	135,762	0.8618	34,597	0.9299	239,376	0.9762
SVM	151,990	0.8264	189,341	0.5866	71,027	0.6888	284,025	0.7006
FFNN	87,355	0.9502	135,947	0.3274	54,627	0.6389	216,792	0.9190
LSTM	194,191	0.7484	213,229	0.7601	30,719	0.9097	242,091	0.9515

For adjustable load forecasting, LSTM provides the lowest RMSE, whereas RF yields a slightly higher correlation coefficient. This result suggests that LSTM improves point-wise prediction accuracy, while RF remains competitive in preserving the general trend of condition-dependent adjustable loads. For fixed load forecasting, FFNN achieves the lowest RMSE value, whereas RF and LSTM provide the highest correlation coefficients. This indicates that although FFNN reduces the absolute prediction error for relatively stable fixed loads, RF and LSTM better preserve the temporal structure and continuity of the load trajectories. Overall, the results demonstrate that fixed loads are generally easier to estimate than shiftable loads due to their more deterministic consumption characteristics.

Table 4. Test set performance comparison of forecasting models.

Method	RMSE (Fixed)	*R* (Fixed)	RMSE (Shiftable)	*R* (Shiftable)	RMSE (Adjustable)	*R* (Adjustable)	RMSE (Total)	*R* (Total)
RF	220,175	0.9936	157,020	0.7387	40,501	0.9164	335,439	0.9592
SVM	133,103	0.7621	333,576	−0.4537	84,354	0.4064	601,953	−0.4177
FFNN	108,903	0.8957	500,825	−0.3978	72,825	0.2519	319,034	0.8029
LSTM	200,641	0.9938	47,027	0.9733	28,868	0.9146	254,212	0.9901

Another important observation from Table 4 is the weak generalization behavior of SVM and FFNN for shiftable load forecasting. Both methods produce negative correlation coefficients for shiftable load, while SVM also generated a negative correlation value for total load forecasting. These results indicate that the corresponding models are unable to adequately preserve the temporal structure of highly dynamic residential load components on previously unseen data.

This limitation is particularly pronounced for shiftable loads, whose activation patterns are strongly event-driven and highly dependent on user scheduling behavior. Due to the smoothing nature of kernel-based regression, the SVM model tends to average abrupt temporal variations, thereby reducing its ability to represent sharp transitions and intermittent activation patterns. Similarly, the FFNN architecture, which processes each time step independently without explicit temporal memory, exhibits difficulties in capturing sequential dependencies in minute-level load data.

By contrast, the sliding-window LSTM model maintains consistently high positive correlation values across all load categories, demonstrating its superior capability in preserving temporal continuity, sequential structure, and dynamic consumption behavior. These findings highlight the importance of sequence-aware forecasting architectures for high-resolution residential load prediction problems.

The training set metrics further support these observations. RF and LSTM achieved very low training RMSE values together with extremely high correlation coefficients, indicating strong learning capability for both structured and sequential residential load patterns. FFNN also demonstrates relatively stable performance for fixed load forecasting; however, its performance degrades substantially for shiftable and adjustable loads, suggesting limited capability in modeling highly dynamic temporal variations without recurrent memory mechanisms. The numerical findings demonstrate that the sliding-window LSTM architecture is the most effective approach for capturing strongly time-dependent residential load behavior, while RF remains highly competitive for relatively structured and condition-driven outputs.

The MAE results presented in Table 5 further confirm the superiority of the LSTM model in terms of average prediction accuracy. Unlike RMSE, which emphasizes larger forecasting deviations, MAE reflects the average magnitude of absolute prediction errors. The consistently lower MAE values obtained by the LSTM model across all load categories indicate that the proposed sequence-aware architecture achieves not only improved temporal tracking performance but also more stable point-wise estimation accuracy.

Table 5. Test set MAE comparison of forecasting models.

Method	MAE (Fixed)	MAE (Shiftable)	MAE (Adjustable)	MAE (Total)
RF	210,911	90,373	26,746	306,277
SVM	112,680	274,235	65,458	368,742
FFNN	126,068	519,631	48,576	656,487
LSTM	97,258	32,767	17,686	131,851

To further evaluate short-term forecasting behavior, an additional bus-wise analysis is conducted over a three-day interval covering Days 26–28. Since the dataset contains multiple bus level observations, combining all buses within a single temporal sequence may obscure the localized dynamics of individual buses. Therefore, the short-window analysis is performed separately for each bus, and the forecasting results are visualized using a 2×2 layout including fixed, shiftable, adjustable, and total load components. For each bus, the corresponding actual and predicted trajectories are compared over the selected interval, and bus-specific RMSE and correlation values are computed for all four outputs.

The resulting bus-wise numerical results are reported in Tables 6–9. In this analysis, each bus contributed 4320 samples, corresponding to a complete three-day interval at one-minute resolution. The short-window results reveal that local forecasting behavior differs across buses, reflecting the spatial heterogeneity of residential demand in the distribution system.

The bus-wise short-window analysis provides a more localized interpretation of model behavior than the global test metrics alone. The obtained results indicate that forecasting performance varies considerably depending on both the bus characteristics and the load category under consideration. For Buses 1 and 2, the RF model consistently achieved the lowest RMSE values across all four load categories. In these buses, RF also maintains near-perfect correlation coefficients, demonstrating excellent short-horizon tracking capability under relatively regular and repetitive local demand conditions. These findings suggest that tree-based partitioning methods are highly effective when local load behavior remains relatively stable over short forecasting intervals.

The results for Bus 3 exhibit a more heterogeneous behavior. RF achieves the best performance for fixed and adjustable loads, whereas FFNN yielded the lowest RMSE for shiftable load forecasting. In contrast, the LSTM model provided the lowest RMSE for total load forecasting. This variation indicates that no single forecasting architecture universally dominates all load components when local demand dynamics become more irregular and spatially heterogeneous.

Table 6. Bus-wise short-window forecasting performance for Bus 1 over Days 26–28.

Method	RMSE (Fixed)	*R* (Fixed)	RMSE (Shiftable)	*R* (Shiftable)	RMSE (Adjustable)	*R* (Adjustable)	RMSE (Total)	*R* (Total)
RF	10,546	0.9982	13,438	0.9994	13,413	0.9785	23,471	0.9990
SVM	93,518	0.9671	97,382	0.9839	32,126	0.9004	152,824	0.9876
FFNN	93,781	0.8972	165,631	0.9538	60,451	0.5129	287,777	0.9275
LSTM	27,060	0.9885	45,050	0.9930	31,336	0.8848	60,183	0.9936

Table 7. Bus-wise short-window forecasting performance for Bus 2 over Days 26–28.

Method	RMSE (Fixed)	*R* (Fixed)	RMSE (Shiftable)	*R* (Shiftable)	RMSE (Adjustable)	*R* (Adjustable)	RMSE (Total)	*R* (Total)
RF	12,226	0.9989	14,227	0.9997	19,424	0.9861	28,705	0.9994
SVM	81,990	0.9580	106,300	0.9891	38,401	0.9480	129,305	0.9911
FFNN	124,931	0.8890	183,620	0.9584	87,777	0.6699	309,342	0.9318
LSTM	38,431	0.9903	49,660	0.9964	38,514	0.9436	72,639	0.9962

Table 8. Bus-wise short-window forecasting performance for Bus 3 over Days 26–28.

Method	RMSE (Fixed)	*R* (Fixed)	RMSE (Shiftable)	*R* (Shiftable)	RMSE (Adjustable)	*R* (Adjustable)	RMSE (Total)	*R* (Total)
RF	47,689	0.9976	224,164	0.9067	29,508	0.9479	189,152	0.9850
SVM	110,578	0.9557	202,874	0.8197	61,413	0.8969	298,981	0.9320
FFNN	297,414	0.8490	400,393	0.5927	68,811	0.6586	245,391	0.8743
LSTM	46,936	0.9893	47,135	0.8893	32,045	0.9131	79,620	0.9782

Table 9. Bus-wise short-window forecasting performance for Bus 4 over Days 26–28.

Method	RMSE (Fixed)	*R* (Fixed)	RMSE (Shiftable)	*R* (Shiftable)	RMSE (Adjustable)	*R* (Adjustable)	RMSE (Total)	*R* (Total)
RF	245,662	0.9963	263,331	0.8936	46,640	0.9306	443,137	0.9812
SVM	152,942	0.9605	363,219	−0.1113	109,183	0.4735	336,195	−0.0638
FFNN	438,593	0.6726	407,987	0.1441	162,814	0.5754	1,570,703	0.2256
LSTM	130,751	0.9819	49,063	0.8716	41,920	0.8176	227,834	0.9795

For Bus 4, the LSTM model becomes significantly more advantageous, particularly for shiftable, adjustable, and total load forecasting. In this bus, LSTM achieved substantially lower RMSE values together with very high correlation coefficients, indicating that recurrent memory-based learning becomes increasingly beneficial under highly dynamic and event-driven residential load conditions. Although SVM yielded the lowest RMSE for fixed load forecasting in Bus 4, its negative correlation values for shiftable and total load demonstrate weak temporal generalization capability for more complex demand patterns.

The corresponding short-window visualizations for Buses 1–4 are presented in Figures 11–14. These visual results are consistent with the numerical findings reported in Tables 6–9. In general, RF demonstrates highly accurate short-term tracking performance for buses with relatively repetitive local demand patterns, whereas the LSTM model more effectively preserves temporal continuity and sequential behavior under increasingly irregular and event-driven operating conditions. The visual comparisons also reveal that shiftable load forecasting constitutes the most challenging prediction task due to the abrupt and user-dependent activation characteristics of these appliances. In this context, sequence-aware architectures such as LSTM provide more stable temporal representations compared to static regression-based approaches.

https://doi.org/10.3390/app16125904

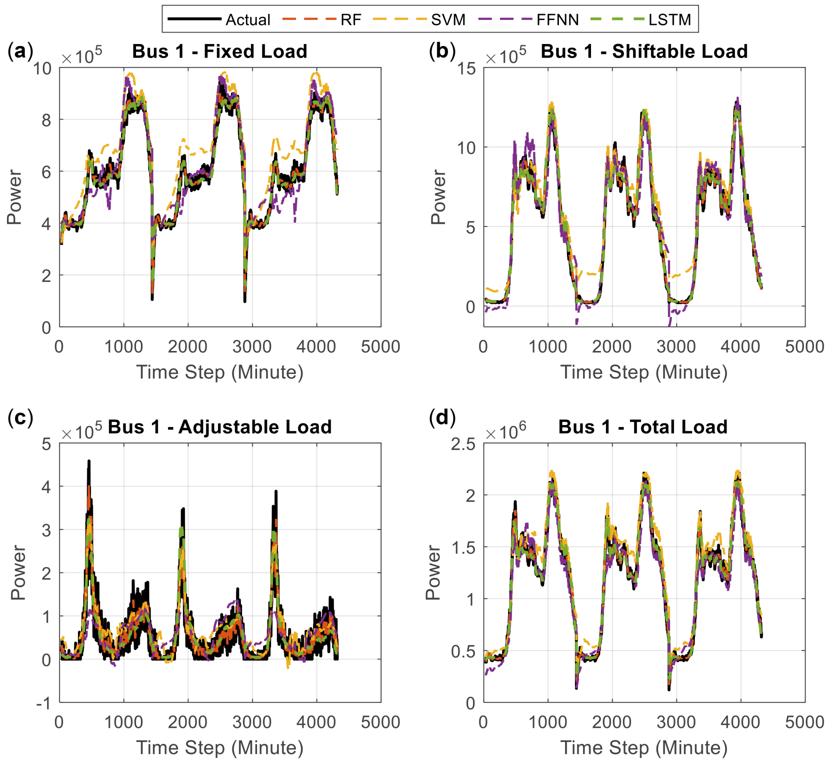

Figure 11. Bus-wise short-window forecasting results for Bus 1 over Days 26–28: (**a**) fixed load, (**b**) shiftable load, (**c**) adjustable load, and (**d**) total load.

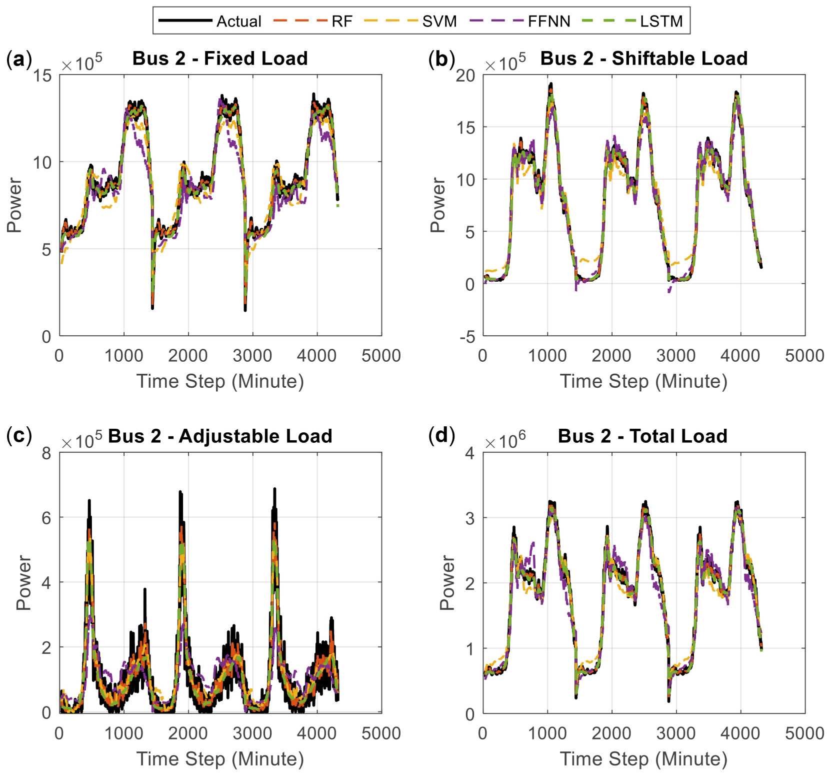

Figure 12. Bus-wise short-window forecasting results for Bus 2 over Days 26–28: (**a**) fixed load, (**b**) shiftable load, (**c**) adjustable load, and (**d**) total load.

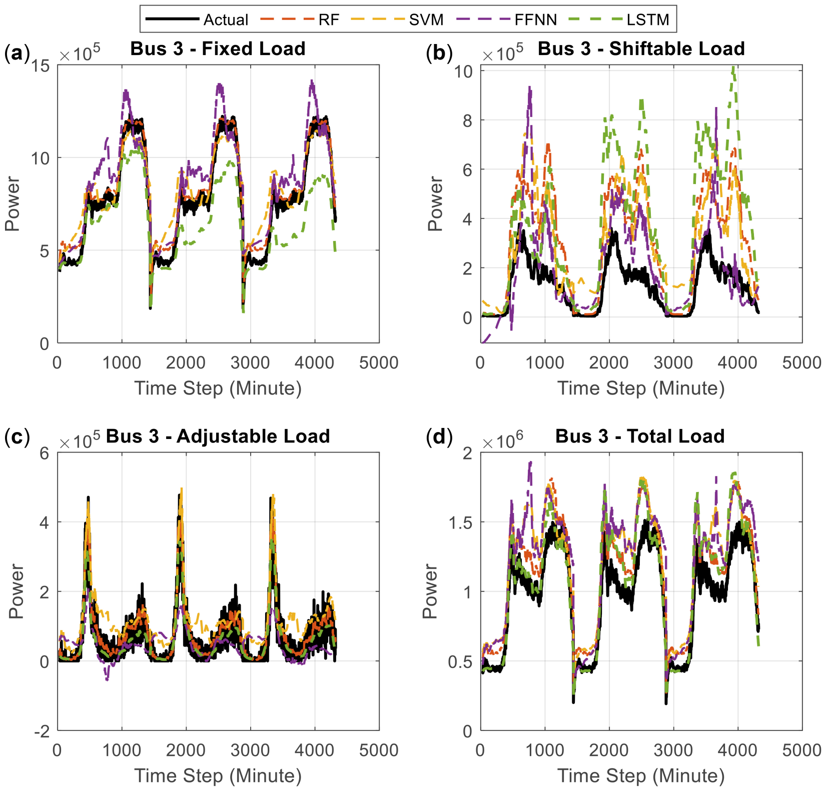

Figure 13. Bus-wise short-window forecasting results for Bus 3 over Days 26–28: (**a**) fixed load, (**b**) shiftable load, (**c**) adjustable load, and (**d**) total load.

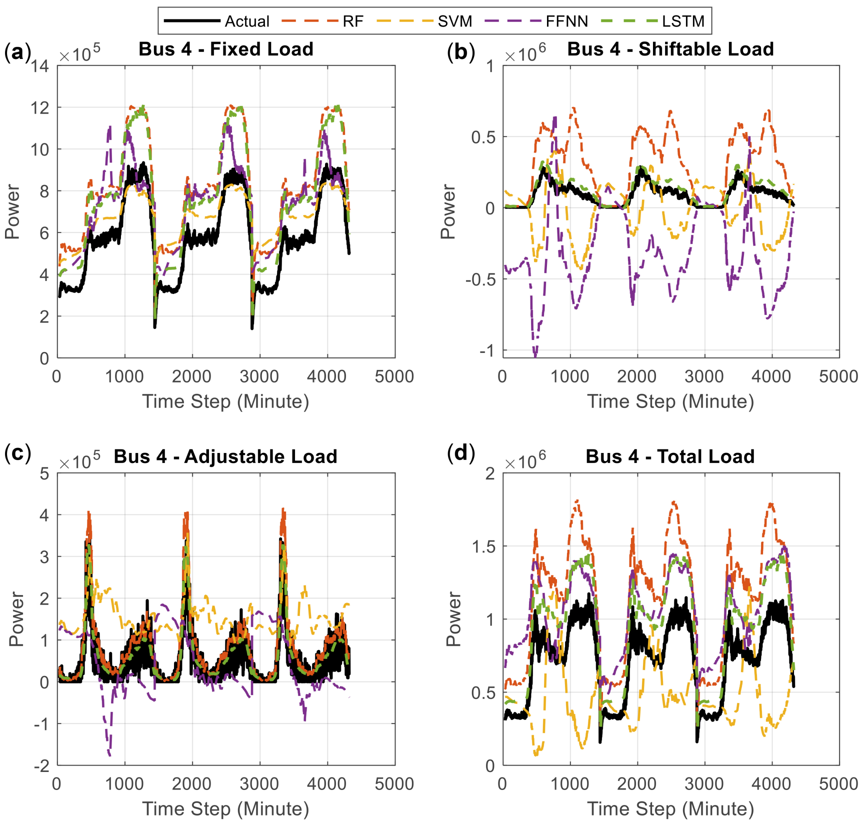

Figure 14. Bus-wise short-window forecasting results for Bus 4 over Days 26–28: (**a**) fixed load, (**b**) shiftable load, (**c**) adjustable load, and (**d**) total load.

4.1. Feature Importance Analysis

To further evaluate the contribution of the input variables to the forecasting process, a feature importance analysis is performed using the out-of-bag permuted predictor importance scores obtained from the random forest models. Since residential demand characteristics may vary spatially across the distribution system, the analysis is conducted specifically for Bus 3, which exhibits relatively heterogeneous load behavior during the forecasting experiments.

As shown in Figure 15, the relative contribution of the input variables differs considerably across the load categories, confirming that each residential load type exhibits distinct temporal and environmental dependencies. For fixed load forecasting, the minute of day variable provides the dominant contribution, indicating that fixed loads mainly follow repetitive intra-day consumption patterns. Technical loss and solar irradiance also exhibit moderate importance, whereas meteorological variables such as temperature and wind speed have relatively weaker effects. This behavior is consistent with the relatively deterministic nature of continuously operating household appliances.

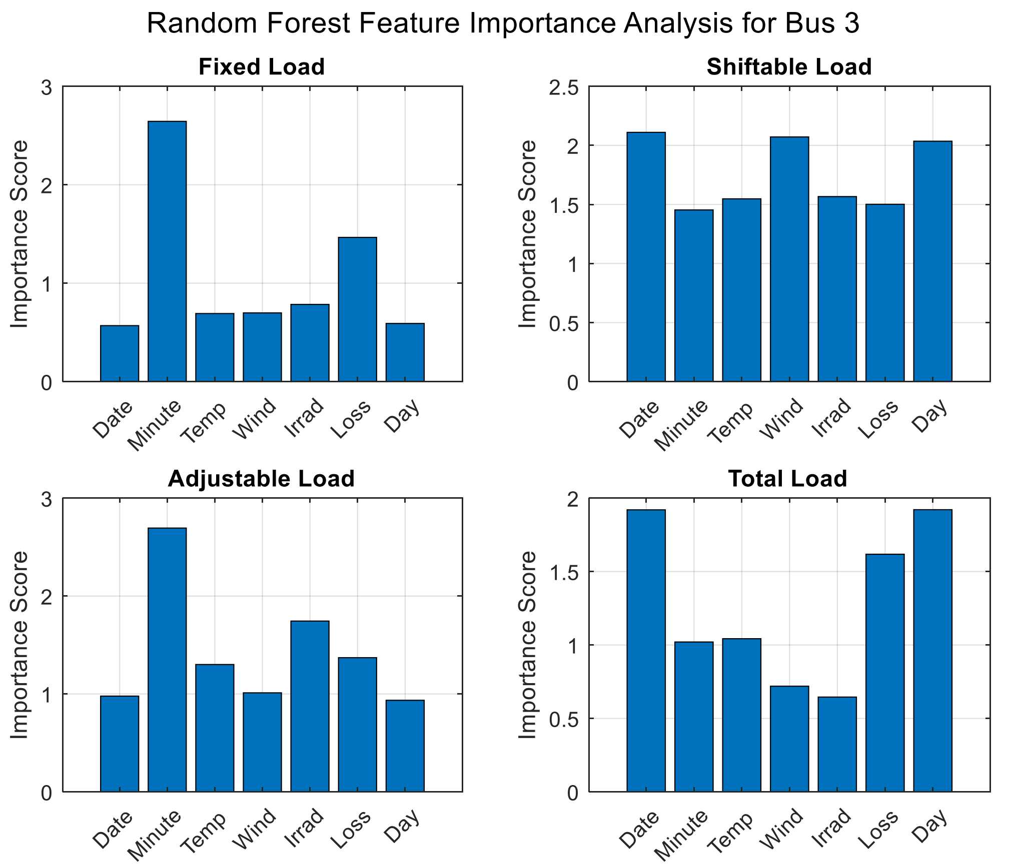

Figure 15. Random forest feature importance analysis for Bus 3 considering fixed, shiftable, adjustable, and total load forecasting outputs.

For shiftable load forecasting, the importance scores are more evenly distributed across the variables. In particular, date, wind speed, and day-related information exhibit relatively strong contributions, suggesting that shiftable loads are influenced by both temporal behavior and user-dependent scheduling patterns. This observation supports the interpretation that shiftable loads constitute the most behaviorally dynamic residential load category.

For adjustable load forecasting, minute of day again provides the highest contribution, while solar irradiance and technical loss also demonstrate substantial importance. Since adjustable loads are largely associated with temperature dependent and controllable appliances, the stronger contribution of environmental variables is physically meaningful and consistent with the operational characteristics of thermal loads.

For total load forecasting, date- and day-related information and technical loss emerge as the most influential variables, indicating that aggregated residential demand is shaped not only by intra-day behavioral patterns but also by longer temporal trends and network operating conditions. The relatively high contribution of technical loss further justifies the inclusion of power-flow-derived network information within the proposed forecasting framework.

4.2. General Discussion

From a broader perspective, the results demonstrate that residential demand cannot be treated as a homogeneous signal if the objective is to obtain high-fidelity forecasts for smart-grid-oriented applications. Each load component exhibits distinct statistical and temporal characteristics, and these differences directly influence the relative success of the forecasting methods. Fixed loads are predominantly deterministic and therefore easier to estimate. Shiftable loads contain stronger temporal uncertainty and require sequential learning capability. Adjustable loads are shaped more by instantaneous exogenous conditions and are therefore relatively more amenable to condition-based regression structures. In this context, the superiority of LSTM in the overall test set analysis and its strong performance in the more challenging bus-wise cases indicate that temporal memory is a decisive advantage when the objective is to forecast multiple residential load components at minute resolution.

These findings also have important implications for demand-side management and flexibility-oriented grid operation. Since fixed loads form the baseline consumption layer, they offer limited responsiveness to control- or price-based interventions. Shiftable loads, on the other hand, provide flexibility on the temporal axis, enabling the postponement or advancement of appliance operation without fundamentally altering the associated energy requirement. Adjustable loads contribute a different type of flexibility by allowing power magnitude modulation under suitable control strategies. Therefore, the decomposition of residential demand into fixed, shiftable, adjustable, and total components provides a much richer analytical basis than aggregate load forecasting alone. The forecasting framework developed in this study can therefore support not only more accurate short-term demand forecasting, but also more informed decision making for dynamic pricing, peak shaving, load shaping, and residential energy management applications.

Overall, the experimental results confirm that the proposed load-type-based forecasting framework is capable of modeling heterogeneous residential demand at minute resolution with a high degree of fidelity. Among the evaluated methods, LSTM provides the strongest overall generalization capability, especially for shiftable and total load forecasting, whereas RF offers excellent short-window performance under relatively regular local operating conditions. SVM and FFNN, although partially effective for certain structured outputs, are not sufficiently robust across all load components and buses. These results indicate that when appliance-level aggregation, meteorological variables, temporal indices, bus-level spatial information, and technical losses are jointly considered, sequence-aware deep learning methods provide the most suitable architecture for high-resolution residential-load-type forecasting.

4.3. Impact of Load Categorization on Forecasting Performance

To further investigate the impact of load categorization on forecasting performance, an additional analysis is conducted using the LSTM model. In this analysis, total load is predicted directly using a single model, and the results are compared with the categorized forecasting approach, where fixed, shiftable, and adjustable loads are predicted separately and then aggregated.

A comparative analysis reveals that direct total load forecasting achieves a lower RMSE (110,032.70), whereas the categorized approach yields a higher correlation coefficient ($R = 0.9848$) compared to the direct model ($R = 0.9683$).

This comparison suggests that although load categorization does not necessarily minimize point-wise prediction error (as reflected by RMSE), it enhances the model's ability to capture temporal dependencies and structural patterns in residential electricity demand.

From an application perspective, this distinction is particularly important for demand-side management, where accurately capturing load behavior and variability can be more relevant than minimizing absolute numerical error. Therefore, the categorized forecasting framework provides a more informative and interpretable representation of residential demand. This advantage is particularly relevant for flexibility-oriented applications such as demand response and dynamic pricing, where accurately capturing load behavior is more critical than minimizing absolute prediction error.

4.4. Limitations and Generalizability

Although the CREST-based dataset provides a reproducible and privacy-preserving platform for evaluating load-type-based forecasting, the reliance on synthetic data constitutes an inherent limitation of this study. Synthetic profiles may not fully reflect real-world consumption variability, including behavioral uncertainty, socio-economic diversity, and unexpected usage patterns. Furthermore, replicating the proposed framework using real-world data would require detailed appliance-level load decomposition for each household as well as complete knowledge of the distribution network structure, which are often difficult to obtain in a comprehensive and fully labeled form in practical applications.

In addition, the dataset used in this study covers only a winter period (January), and therefore does not capture seasonal variations in residential demand behavior, particularly for temperature-dependent loads such as heating and cooling. As a result, the generalization of the proposed framework across different seasons requires further investigation.

Another limitation arises from the use of a single distribution system (Civanlar test network). Although this system provides a realistic and widely accepted benchmark structure, different network topologies, load compositions, and regional consumption patterns may influence forecasting performance. This limitation is particularly relevant for flexibility-oriented applications such as demand response and dynamic pricing, where understanding load behavior is more critical than minimizing absolute prediction error. Therefore, future work will focus on validating the proposed framework using real-world datasets and evaluating its robustness under practical operating conditions.

5. Conclusions

This study proposes a load-type-based short-term residential load forecasting framework in which total household demand is decomposed into fixed, shiftable, and adjustable components. A high-resolution dataset is generated using the CREST model and integrated with meteorological variables, temporal indicators, and technical loss information within a unified multi-input forecasting structure.

The results demonstrate that residential electricity demand cannot be accurately represented as a single aggregated signal, as each load category exhibits distinct temporal and statistical characteristics. Among the evaluated forecasting approaches, the sliding-window LSTM model provides the most consistent overall performance, particularly for temporally dynamic load components. Specifically, LSTM achieve RMSE values of 47,027, 28,868, and 254,212 for shiftable, adjustable, and total load forecasting, respectively, with corresponding correlation coefficients of $R = 0.9733$, $R = 0.9146$, and $R = 0.9901$. In terms of MAE, LSTM also achieved the lowest average absolute errors across all load categories, with MAE values of 97,258, 32,767, 17,686, and 131,851 for fixed, shiftable, adjustable, and total load, respectively.

The RF model also demonstrated highly competitive performance, particularly under localized short-window forecasting conditions in Buses 1 and 2, where repetitive and relatively stable demand patterns were dominant. In contrast, SVM and FFNN exhibited weaker generalization capability for highly dynamic load categories, especially for shiftable loads characterized by abrupt user-driven activation behavior.

Beyond forecasting accuracy, the proposed decomposition framework provides a more informative representation of residential demand behavior. Fixed loads define the baseline consumption, while shiftable and adjustable loads reveal the flexibility potential of households in terms of temporal rescheduling and power modulation. This distinction is critical for understanding and quantifying demand-side flexibility in modern distribution systems. The proposed categorized forecasting framework therefore establishes a direct analytical link between high-resolution load forecasting and demand-side management applications. In particular, the ability to separately forecast shiftable and adjustable loads enables the identification of controllable demand segments that can be targeted through demand response strategies. These outputs can be directly utilized to design time-dependent pricing signals, schedule flexible appliance operation, and implement peak load reduction strategies in a more structured and data-driven manner.

Building on this foundation, future work will focus on integrating the proposed load-type forecasting framework with demand response optimization models. In particular, forecasted shiftable loads can be used to determine optimal load shifting schedules, while adjustable loads can be incorporated into real-time control schemes for power modulation. In addition, coupling the proposed framework with dynamic pricing mechanisms and user comfort constraints is expected to enable the development of practical and scalable residential energy management systems.

Author Contributions: Conceptualization, E.O., U.S.S. and İ.G.T.; methodology, E.O.; software, E.O.; validation, E.O. and U.S.S.; formal analysis, E.O. and İ.G.T.; investigation, E.O.; resources, U.S.S. and İ.G.T.; data curation, E.O.; writing—original draft preparation, E.O.; writing—review and editing, U.S.S. and İ.G.T.; visualization, E.O.; supervision, U.S.S. and İ.G.T.; project administration, U.S.S. and İ.G.T. All authors have read and agreed to the published version of the manuscript.

Funding: This research received no external funding.

Institutional Review Board Statement: Not applicable.

Informed Consent Statement: Not applicable.

Data Availability Statement: The data that support the findings of this study are available on request from the corresponding authors.

Conflicts of Interest: The authors declare no conflicts of interest.

Abbreviations

The following abbreviations are used in this manuscript:

STLF	Short-term load forecasting
CREST	Centre for Renewable Energy Systems Technology
DSM	Demand-side management
DR	Demand response
MIMO	Multi-input multi-output

RF	Random forest
SVM	Support vector machine
SVR	Support vector regression
FFNN	Feed-forward neural network
LSTM	Long short-term memory
RNN	Recurrent neural network
RMSE	Root mean square error
MAE	Mean absolute error
BPTT	Backpropagation through time
SCG	Scaled conjugate gradient
RBF	Radial basis function

Appendix A. CREST Model Details

The CREST (Centre for Renewable Energy Systems Technology) model is a stochastic demand model widely used for the generation of high-resolution residential electricity consumption profiles.

The model simulates household electricity usage by representing appliance-level behavior through probabilistic rules. Appliance operation is influenced by occupancy patterns and predefined usage characteristics, enabling realistic modeling of daily consumption behavior.

The model generates appliance-level electricity consumption data at a one-minute resolution. Each appliance is modeled individually, and the total residential electricity demand is obtained by aggregating the contributions of all appliances over time.

Within the generated dataset, appliance-level loads can be grouped based on their operational flexibility into three main categories:

- Fixed loads: Appliances with continuous or inflexible operation that form the baseline demand.
- Shiftable loads: Appliances whose operation can be shifted in time without significantly affecting their functionality.
- Adjustable loads: Flexible loads that can be controlled or adjusted depending on external conditions or control strategies.
  This categorization supports the analysis of different load types within the forecasting framework. The stochastic structure of the CREST model introduces variability across households and time periods, resulting in diverse and realistic load profiles suitable for demand forecasting applications.

References

1. Wang, Y.; Zhang, N.; Chen, X. A short-term residential load forecasting model based on LSTM recurrent neural network considering weather features. *Energies* **2021**, *14*, 2737. [CrossRef]
2. Fagundes, S.; Cardoso, F.; Stangler, E.; Neves, F.; Mezaroba, M. A detailed power flow analysis of the dual unified power quality conditioner (iUPQC) using power angle control (PAC). *Electr. Power Syst. Res.* **2021**, *192*, 106933. [CrossRef]
3. Kong, W.; Dong, Z.Y.; Jia, Y.; Hill, D.J.; Xu, Y.; Zhang, Y. Short-term residential load forecasting based on LSTM recurrent neural network. *IEEE Trans. Smart Grid* **2019**, *10*, 841–851. [CrossRef]
4. Rafi, S.H.; Deeba, S.R.; Hossain, E. A short-term load forecasting method using integrated CNN and LSTM network. *IEEE Access* **2021**, *9*, 32436–32448. [CrossRef]
5. Dos Reis, F.B.; Tonkoski, R.; Bhattarai, B.P.; Hansen, T.M. A Real-World Test Distribution System with Appliance-Level Load Data for Demand Response and Transactive Energy Studies. *IEEE Access* **2021**, *9*, 149506–149519. [CrossRef]
6. Manembu, P.D.; Kewo, A.; Bramstoft, R.; Nielsen, P.S. A systematicity review on residential electricity load-shifting at the appliance level. *Energies* **2023**, *16*, 7828. [CrossRef]
7. Rodrigues, F.; Cardeira, C.; Calado, J.M.F.; Melício, R. Short-Term Load Forecasting of Electricity Demand for the Residential Sector Based on Modelling Techniques: A Systematic Review. *Energies* **2023**, *16*, 4098. [CrossRef]

8. Patsakos, I.; Vrochidou, E.; Papakostas, G.A. A Survey on Deep Learning for Building Load Forecasting. *Math. Probl. Eng.* **2022**, *2022*, 1008491. [CrossRef]
9. Moradzadeh, A.; Mohammadi-Ivatloo, B.; Abapour, M.; Anvari-Moghaddam, A.; Roy, S.S. Heating and Cooling Loads Forecasting for Residential Buildings Based on Hybrid Machine Learning Applications: A Comprehensive Review and Comparative Analysis. *IEEE Access* **2022**, *10*, 2196–2215. [CrossRef]
10. Zhang, L.; Tang, Y.; Zhou, T.; Tang, C.; Liang, H.; Zhang, J. Research on flexible smart home appliance load participating in demand side response based on power direct control technology. *Energy Rep.* **2022**, *8*, 424–434. [CrossRef]
11. Sahrane, S.; Adnane, M.; Haddadi, M. Multi-label load disaggregation in presence of non-targeted loads. *Electr. Power Syst. Res.* **2021**, *199*, 107435. [CrossRef]
12. Hayn, M.; Zander, A.; Fichtner, W.; Nickel, S.; Bertsch, V. The impact of electricity tariffs on residential demand side flexibility: Results of bottom-up load profile modeling. *Energy Syst.* **2018**, *9*, 759–792. [CrossRef]
13. Sharma, M.; Mittal, N.; Mishra, A.; Gupta, A. Survey of Electricity Demand Forecasting and Demand Side Management Techniques in Different Sectors to Identify Scope for Improvement. *Smart Grids Sustain. Energy* **2023**, *8*, 9. [CrossRef]
14. Gao, B.; Liu, X.; Zhu, Z. A Bottom-Up Model for Household Load Profile Based on the Consumption Behavior of Residents. *Energies* **2018**, *11*, 2112. [CrossRef]
15. Kewo, A.; Manembu, P.D.K.; Nielsen, P.S. A Rigorous Standalone Literature Review of Residential Electricity Load Profiles. *Energies* **2023**, *16*, 4072. [CrossRef]
16. Fischer, D.; Surmann, A.; Biener, W.; Selinger-Lutz, O. From residential electric load profiles to flexibility profiles—A stochastic bottom-up approach. *Energy Build.* **2020**, *224*, 110133. [CrossRef]
17. Claeys, R.; Cleenwerck, R.; Knockaert, J.; Desmet, J. Capturing multiscale temporal dynamics in synthetic residential load profiles through Generative Adversarial Networks (GANs). *Appl. Energy* **2024**, *360*, 122831. [CrossRef]
18. Claeys, R.; Cleenwerck, R.; Knockaert, J.; Desmet, J. Stochastic generation of residential load profiles with realistic variability based on wavelet-decomposed smart meter data. *Appl. Energy* **2023**, *350*, 121750. [CrossRef]
19. Pachanapan, P.; Trairat, P.; Kanprachar, S. Synthetic Domestic Electricity Demand in Thailand Using A Modified High Resolution Modelling Tool by CREST. *ECTI Trans. Electr. Eng. Electron. Commun.* **2021**, *19*, 145–154. [CrossRef]
20. De Paola, A.; Fortunati, L.; Musiari, E.; Anselmi, G.P.; Currò, D.; Andreadou, N.; Kotsakis, E.; Fulli, G. Residential load forecast: An enhanced machine learning model with socio-economic data and synthetic features. *Results Eng.* **2026**, *29*, 109184. [CrossRef]
21. Ma, P.; Cui, S.; Chen, M.; Zhou, S.; Wang, K. Review of family-level short-term load forecasting and its application in household energy management system. *Energies* **2023**, *16*, 5809. [CrossRef]
22. Yildiz, B.; Bilbao, J.I.; Sproul, A.B. A review and analysis of regression and machine learning models on commercial building electricity load forecasting. *Renew. Sustain. Energy Rev.* **2017**, *73*, 1104–1122. [CrossRef]
23. Green, C.; Garimella, S. Very low-resolution residential load disaggregation with unsupervised graph signal processing. *Electr. Power Syst. Res.* **2023**, *215*, 108998. [CrossRef]
24. Nikolaidis, P. Smart Grid Forecasting with MIMO Models: A Comparative Study of Machine Learning Techniques for Day-Ahead Residual Load Prediction. *Energies* **2024**, *17*, 5219. [CrossRef]
25. Abujubbeh, M.; Natarajan, B. Overview of loss sensitivity analysis in modern distribution systems. *IEEE Access* **2022**, *10*, 16037–16051. [CrossRef]
26. Wang, C.; Zhao, H.; Liu, Y.; Fan, G. Minute-level ultra-short-term power load forecasting based on time series data features. *Appl. Energy* **2024**, *372*, 123801. [CrossRef]
27. Richardson, I.; Thomson, M.; Infield, D.; Clifford, C. Domestic electricity use: A high-resolution energy demand model. *Energy Build.* **2010**, *42*, 1878–1887. [CrossRef]
28. Civanlar, S.; Grainger, J.J.; Yin, H.; Lee, S.S.H. Distribution Feeder Reconfiguration for Loss Reduction. *IEEE Trans. Power Deliv.* **1988**, *3*, 1217–1223. [CrossRef]
29. Tekdemir, İ.G. Dağıtım Sistemlerinde Durum Kestirimi için İstatistiksel Bir Yaklaşım. In Proceedings of the ELECO 2022 Electrical and Electronics Engineering Conference, ELECO, Virtual, 24–26 November 2022; pp. 1–5.
30. Ji, Y.; Buechler, E.; Rajagopal, R. Data-driven load modeling and forecasting of residential appliances. *IEEE Trans. Smart Grid* **2020**, *11*, 2652–2661. [CrossRef]
31. Dewangan, C.L.; Vijayan, V.; Shukla, D.; Chakrabarti, S.; Singh, S.; Sharma, A.; Hossain, M.A. An improved decentralized scheme for incentive-based demand response from residential customers. *Energy* **2023**, *284*, 128568. [CrossRef]
32. Wang, C.; Liu, C.; Lin, Y.; Bi, T. Day-ahead dispatch of integrated electric-heat systems considering weather-parameter-driven residential thermal demands. *Energy* **2020**, *203*, 117847. [CrossRef]
33. Zippenfenig, P. *Open-Meteo.com Weather API*; Zenodo: Geneva, Switzerland, 2024. [CrossRef]

34. Calgan, H. Optimal C-type filter design for wireless power transfer system by using support vector machines. *Int. J. Optim. Control Theor. Appl.* **2023**, *13*, 151. [CrossRef]
35. Hochreiter, S.; Schmidhuber, J. Long short-term memory. *Neural Comput.* **1997**, *9*, 1735–1780. [CrossRef] [PubMed]